

Orientationally ordered aggregates of stiff polyelectrolytes in the presence of multivalent salt

Sarah Mohammadinejad

Institute for Advanced Studies in Basic Sciences (IASBS), P. O. Box 45195-1159,
Zanjan 45195, Iran. E-mail: sarah@iasbs.ac.ir

Hossein Fazli

Institute for Advanced Studies in Basic Sciences (IASBS), P. O. Box 45195-1159,
Zanjan 45195, Iran. E-mail: fazli@iasbs.ac.ir

Ramin Golestanian

Department of Physics and Astronomy, University of Sheffield,
Sheffield S3 7RH, UK. E-mail: r.golestanian@sheffield.ac.uk

Received XXXXth Month, 200X

Accepted XXXXth Month, 200X

DOI: 10.1039/

Aggregation of stiff polyelectrolytes in solution and angle- and distance-dependent potential of mean force between two like-charged rods are studied in the presence of 3-valent salt using molecular dynamics simulations. In the bulk solution, formation of long-lived metastable structures with similarities to the raft-like structures of actin filaments is observed within a range of salt concentration. The system finally goes to a state with lower free energy in which finite-sized bundles of parallel polyelectrolytes form. Preferred angle and interaction type between two like-charged rods at different separations and salt concentrations are also studied, which shed some light on the formation of orientationally ordered structures.

1 Introduction

It is well known that highly charged anionic biological polyelectrolytes such as DNA and filamentous actin (F-actin) could attract each other in the presence of multivalent cations [1].

Attraction between similarly charged polyelectrolytes, which is due to electrostatic correlations and can not be described in the framework of mean field theories such as Poisson-Boltzmann formalism, has been the subject of intense ongoing investigations in the past few decades [1, 2, 3, 4, 5, 6, 7, 8, 9, 10, 11, 12, 13]. Aggregation of stiff polyelectrolytes in solution in the presence of multivalent salt arises from such like-charge attractions.

Depending on their different roles in the cell function, actin filaments assemble into networks (large crossing angle) or bundles (nearly parallel), respectively, helped by bundling or cross-linking proteins [14]. A similar pattern—namely, formation of both networks and dense bundles—has also been observed experimentally in solutions of F-actin rods with multivalent salt, depending on the salt concentration [15]. In a particular range of salt concentrations, a multi-axial liquid crystalline phase of actin rods has been observed in which aggregates resembling stacks of raft-like structures form. These structures, which consist of a com-

combination of mutually parallel and perpendicular F-actin rods, change to bundles of parallel rods with increasing multivalent salt concentration [15]. This is a manifestation of the rich complexity of high density aggregates of linear polyelectrolytes due to *frustration* in accommodating strong electrostatic interactions and geometrical constraints simultaneously. Similar effects arising from electrostatic frustration have been studied theoretically in the context of rodlike polyelectrolyte aggregates [16], rodlike polyelectrolyte brushes [17], and star polyelectrolytes [18].

Formation of novel raft-like aggregates of actin rods in the presence of multivalent salt has been studied both theoretically and using computer simulation methods. As a model system, nematic mixture of rigid rods and strong $\frac{\pi}{2}$ cross-linkers has been studied theoretically using Onsager excluded volume theory, and the possibility of formation of stacks of raft-like structures has been shown [19]. Distance-dependent interaction between two parallel similarly charged rigid rods in the presence of explicit mono- and multivalent salt ions and angle-dependent interaction between them at close center-to-center separation have been studied by Lee *et al.* using molecular dynamics (MD) simulations [20]. In their study, Lee *et al.* have shown that just above the threshold value of multivalent salt concentration needed for attraction between parallel rods, the preferred angle at close separations is 90° , and they have concluded that this is in agreement with formation of raft-like structures in multivalent salt solution of F-actin rods.

The phase behavior of a model system composed of similarly charged rigid rods and inter-rod linkers has also been studied using Debye-Hückel theory of electrostatic interaction between the rods and considering the role of the linkers in the effective inter-rod interaction potential [21]. In this study, it has been shown that aggregates with different orientational orderings of the rods can be formed at different values of rod and linker concentrations. Recently, aggregation of stiff polyelectrolytes has been studied using MD simulations in the presence of multivalent counterions [22] and in the

multivalent salt solution [23]. In Ref. [23] it is shown that the dominant kinetic mode in aggregation process is the case of one end of one rod meeting others at right angle with no appreciable energy barrier and the polyelectrolytes have a tendency to form finite-sized bundles. The kinetics of aggregation and bundle formation of actin has also been recently probed experimentally [24]. Using two different fluorescently labeled populations of F-actin, it was shown that the growth mode of actin bundles in the late stages is predominantly longitudinal, and that the bundles can freely exchange filaments with the solution and therefore are not in a frozen state [24]. It was also found that the energy barrier for the aggregation process is negligibly small (of the order of $k_B T$) [24] in agreement with the theoretical result of Ref. [23].

Considering the complexity of the problem of highly charged rod-like polyelectrolytes at high densities, it seems that more studies are needed to fully unravel the dynamic behavior of the system. Here we use a combination of simulation of the bulk solution of stiff polyelectrolytes and calculation of the effective interaction potential between a pair of polyelectrolytes in the presence of multivalent salt to better understand the orientational ordering of the polyelectrolytes in the aggregation process. We use MD simulations to study stiff polyelectrolytes in the bulk solution in the presence of explicit counter-ions and ions of multivalent salt. We also examine the angle- and distance-dependent potential of mean force between two similarly charged rigid rods in the presence of multivalent salt to help understand the observations of the bulk solution simulations. We find that there could be *three* different regimes in the aggregation behavior of stiff polyelectrolytes in a multivalent salt solution, depending the salt concentration. When the salt concentration is low, the system does not undergo aggregation because the attraction between polyelectrolytes is not strong enough to trigger it. In an intermediate range of salt concentrations, relatively long-lived structures with special orientational ordering of polyelectrolytes form. In these scaffold-like structures, polyelectrolytes are predominantly joined either parallel or perpendicular to each other (see Fig.

1), which is presumably due to the dominant kinetic mode of aggregation [23]. After sufficiently long time, however, mutually perpendicular rods in each structure slide against each other and join up in parallel, such that eventually bundles of parallel polyelectrolytes form. These meta-stable structures have similarities to the raft-like structures of actin filaments observed experimentally [15]. In the high salt concentration regime, the polyelectrolytes directly aggregate into bundles of parallel rods and do not exhibit right-angle configurations in their kinetic pathway of aggregation.

We also calculate the angle- and distance-dependent potential of mean force between two similarly charged rigid rods, and find that in the low salt concentration regime there is no attraction between rods. In the regime with intermediate values of salt concentration, the interaction between parallel rods is attractive but in a range of center-to-center separation where the preferred angle between the rods is 90° . In this regime, the parallel configuration is preferred only at very close separations. In the high salt concentration regime, the parallel configuration is preferred at all separations and the interaction between parallel rods is attractive.

We also check the stability (life-time) of raft-like structures by constructing such structures and monitoring their subsequent evolution as shown in Fig. 2, at different values of salt concentration. We find that these structures are not stable in the low and high salt concentration regimes: while at low salt concentrations mutual repulsion between rods destroys such structures, at high salt concentrations mutually perpendicular rods slide against each other in a very short time and the raft-like structures change to bundles of parallel rods. In the intermediate salt concentration regime, raft-like structures are relatively long-lived. We have observed that the life time of such structures rapidly increases with the number of rods.

The rest of the paper is organized as follows. In Sec. 2, the simulation method and the results of our studies on the aggregation of polyelectrolytes are explained. Section 3 is devoted to the studies on the potential of mean force between rods at various separations and angles,

while Sec. 4 describes the studies on the stability of raft-like structures. Finally, Sec. 5 concludes the paper.

2 Aggregation of stiff polyelectrolytes in the bulk solution

2.1 The model and the simulation method

In our simulations, which are performed with MD simulation package ESPResSo v.1.8 [25], each polyelectrolyte rod is composed of $N_m = 21$ spherical charged monomers of charge $-e$ (e is electronic charge) and diameter σ . We have considered N_p polyelectrolytes with their monomers being bonded to each other via a FENE [26] (finite extensible non linear elastic) potential, with a the separation between them being fixed at $a = 1.1\sigma$. The bending rigidity of polyelectrolyte chains is modeled with bond angle potential $U_\phi = k_\phi(1 - \cos \phi)$ with $k_\phi = 400k_B T$ in which ϕ is the angle between two successive bond vectors along the polyelectrolyte chain. We use $N_c = N_p \times N_m$ monovalent counter-ions with charge $+e$ to neutralize the polyelectrolyte charges. We also model 3-valent salt as N_{s+} positive ions with charge $+3e$ and $N_{s-} = 3N_{s+}$ negative ions with charge $-e$. We follow Ref. [20] for the definition of salt concentration: $c_{3:1} \equiv N_{s-}/N_c$ (for example $c_{3:1} = 0.5$ means that $N_{s-} = 0.5 \times N_c$). The monomer number density in our simulations is $0.04 \sigma^{-3}$, which is about two times the concentration we have used in Ref. [23]. In addition to long-range Coulomb interaction, we include short-range Lennard-Jones repulsion between particles, which adds an energy scale ϵ and a length scale σ to the system. MD time step in our simulations is $\tau = 0.01 \tau_0$ in which $\tau_0 = \sqrt{\frac{m\sigma^2}{\epsilon}}$ is the MD time scale and m is the mass of the particles. The temperature is fixed at $k_B T = 1.2\epsilon$ using a Langevin thermostat. We use the P3M method to apply periodic boundary conditions for long-range Coulomb interaction in the system. The strength of the elec-

trostatic interaction energy relative to the thermal energy can be quantified by definition of the Bjerrum length $l_B = \frac{e^2}{\epsilon k_B T}$, where ϵ is the dielectric constant of the solvent and in our simulations $l_B = 3.2\sigma$. In water at room temperature $l_B = 7\text{\AA}$ and the value of $l_B = 3.2\sigma$ in our simulations means that $\sigma = 2.2\text{\AA}$ and the separation between charged monomers is $a = 2.5\text{\AA}$. By using the relation for the effective viscosity of the solvent $\eta \simeq 2.4\sqrt{m\epsilon}/\sigma^2$ (from Ref. [27]), we can deduce an estimate for the microscopic time $\tau_0 \simeq \eta\sigma^3/(2k_B T)$. Using the viscosity of water and room temperature, we find $\tau_0 = 1.3$ ps.

In the beginning of bulk solution simulations, we fix the polyelectrolytes in space and leave all the ions to fluctuate around them for 100000 MD time steps, which is enough to equilibrate the ions for every given configuration of the polyelectrolytes. After equilibration, we remove the constraint on the polyelectrolytes and study the aggregation process in the system.

2.2 Results

Our bulk solution simulations show that with changing multivalent salt concentration, three different regimes can exist. At salt concentrations less than a lower value $c_{3:1} \simeq 0.2$ no aggregation is observed in the system. In this regime, the salt concentration is lower than its minimum value needed for like-charge attraction between polyelectrolytes. When a 3-valent salt ion links two monomers from two different polyelectrolytes to each other, thermal fluctuations separate them again and the system does not undergo an aggregation process. At intermediate values of the salt concentration $0.2 \leq c_{3:1} \leq 1.2$, aggregation of polyelectrolytes can be observed and the dominant kinetic mode of aggregation is that of one end of one polyelectrolyte meeting others at a right angle, as previously reported [23]. During the aggregation process in this regime, long-lived structures of polyelectrolytes form, and in each structure polyelectrolytes are dominantly joined either parallel or perpendicular to each other (see Fig. 1 f).

In this regime, after sufficiently long time mutually perpendicular polyelectrolytes in each scaffold-like structure slide against each other

and finally form bundles of parallel polyelectrolytes. The kinetic mode of evolution from scaffold-like structures to bundles is considerably slower than the typical kinetic modes of the system. For example, in a system containing nine polyelectrolytes, the time that takes for the scaffold-like structure (Fig. 1 f) to evolve into the final configuration of a collapsed parallel bundle is greater than the time interval between snapshots *a* and *e* of Fig. 1, by a factor of at least six. This suggests that the formation of long-lived scaffold-like structures corresponds to meta-stable states of the system and the states with bundles of parallel polyelectrolytes have lower free energies. We have checked that the formation of the meta-stable structures is independent of the random number sequence used in the simulation, as well as the initial configuration of the polyelectrolytes. In other words, in the intermediate salt concentration range the relaxation pathway to equilibrium appears to always involve intermediate meta-stable structures. These structures have similarities to the raft-like structures of actin filaments observed experimentally [15] (see below for a discussion). In the regime with high values of salt concentration ($c_{3:1} \geq 1.2$), we observe a different kinetic mode of aggregation in the system. In this regime, the polyelectrolytes directly aggregate into bundles of parallel polyelectrolytes and the salt concentration washes out the right angle configuration from the kinetic pathway of aggregation. The aggregation process in this regime is considerably faster than that of the regime with intermediate salt concentration.

To shed some light on the behavior of the system and better understand these results, we study the potential of mean force between two polyelectrolyte rods.

3 Potential of mean force between charged rods

3.1 The model and the simulation method

In our simulations of two similarly charged rigid rods we consider two rods, each composed of

$N_m = 21$ similarly charged spherical monomers of diameter σ and charge $-e$, $N_c = 2N_m$ counterions of charge $+e$, and 3-valent salt of concentration $c_{3:1}$. The monomer number density in these simulations is $10^{-4} \sigma^{-3}$, which corresponds to a simulation box of length $L \approx 75\sigma$ that is large enough to avoid finite size effects. The rods are fixed on two parallel plates of separation R and the angle between the rods is θ (see the schematic configuration in the inset of the middle part of Fig. 3). For each set of values of R , θ , and $c_{3:1}$, the two rods are fixed during the simulation and only the counterions and the salt ions are free to move. After equilibration of the system we calculate the average force on each monomer and obtain the total force and the total torque around the center-to-center line (y -axis) for one of the rods. We integrate the force with respect to the center-to-center distance, R , to obtain the R -dependence of the potential of mean force, and similarly integrate the torque with respect to the angle θ to obtain its θ -dependence (corresponding to rotation around y -axis). We set the zero of the potential of mean force at $R = 7.5\sigma$ for obtaining its R -dependence, and at $\theta = 90^\circ$ in the calculation of its θ -dependence.

3.2 Results

We first repeat the calculation of the potential of mean force between two parallel rods at different values of salt concentration and center-to-center separation as in Ref. [20]. Our results show that for 3-valent salt concentrations higher than $c_{3:1} = 0.2$, there is attraction between parallel rods (see Fig. 4), in agreement with the results of Ref. [20]. We now consider the following question: if one allows the angle between the rods to vary for other values of R , will the rods prefer to be parallel? To answer this question, we calculate the angle-dependent potential of mean force at different values of R . We find that at the lowest value of R in our simulations, $R = 2.5\sigma$, the preferred angle at salt concentrations less than a threshold value $c_{3:1} \simeq 0.2$ is $\theta = 90^\circ$, and at higher salt concentrations, the parallel configuration is preferred (see $R = 2.5\sigma$ part of Fig. 3). While this is the same result as

reported in Ref. [20], we find that upon increasing R (from $R = 2.5\sigma$), the threshold value of salt concentration below which $\theta = 90^\circ$ is preferred increases (see the parts of Fig. 3 corresponding to $R = 3.5\sigma$ and $R = 4.5\sigma$). These results show that in a range of salt concentrations, if we consider two rod-like polyelectrolytes in the solution at a separation where their effective interaction is appreciable, the interaction potential tends to reorient them to a perpendicular configuration. The preferred orientation is parallel only at very close separations. This could be the origin of the formation of scaffold-like structures in the aggregation of stiff polyelectrolytes. After the formation of such structures, the polyelectrolytes are much closer to each other, and will have a chance to discover that the parallel configuration has a lower free energy, so that perpendicular rods eventually reorient themselves and form bundles.

To elaborate further on this issue, we calculate the distance-dependent potential of mean force between two perpendicular rods, which shows that in the presence of 3-valent salt there can be attractive interaction between them at close separations (see Fig. 5). Moreover, Fig. 5 shows that a barrier exists in the potential of mean force, which decreases with increasing salt concentration. In Ref. [23], it has been shown that the perpendicular configuration of two rods when their ends are close to each other has a lower free energy than the configuration shown in Fig. 5. In fact, within the dominant kinetic mode of aggregation, when two polyelectrolytes are going to join each other with their ends and at right angle, they experience the lowest possible energy barrier. Using the simulation results presented in Figs. 3, 4, and 5, and similar studies at other salt concentrations (not presented here), we have calculated the preferred crossing angle, θ_p , and the interaction type between two rods at different salt concentrations and center-to-center separations as shown in Fig. 6. We find that with increasing salt concentration, the $\theta = \frac{\pi}{2}$ region of the diagram becomes smaller, until it finally vanishes at $c_{3:1} \simeq 1.0$. Moreover, there is a region in the $c_{3:1} - R$ plane for which the preferred angle between the rods is 90° and the interaction is attractive. The existence of

such a regime could explain the formation of the scaffold-like structures during the aggregation of polyelectrolytes. We note that the information extracted from the potential of mean force between a pair of rods on the preferred angle between the rods and whether the interaction is attractive or repulsive does not provide a complete description of the behavior of the system, as the true phase behavior needs to be studied from the global stability (convexity) of the free energy of the system (see e.g. Ref. [28] for such a study in the context of columnar DNA-aggregates). Such a study, however, will involve making assumptions on the structure of the aggregate as studying the full infinite dimensional configuration space of a system of N_p rods is not computationally feasible. Instead, we prefer to use the calculation of the potential of the mean force (which is more tractable) to supplement the results obtained from MD simulations that probe the kinetics of the system while relaxing to equilibrium.

We also calculate the ensemble average of interaction energy (Lennard-Jones + Coulomb) and the potential of mean force (by integration of the torque with respect to the angle) as functions of the angle between rods with monovalent counterions and no added salt. Potential of mean force ΔU is a partial free energy (subject to the constraint that the rods are kept fixed) and can be decomposed into an energetic and an entropic part, namely $\Delta U = \Delta E - T\Delta S$, where the energetic contribution is the average interaction energy ΔE . The potential of mean force ΔU and the average of interaction energy ΔE are shown in Fig. 7. The comparison shows that although the right angle configuration is the preferred form judging from the potential of mean force, the parallel configuration has a lower interaction energy. This could be understood by noting that the counterions in the parallel configuration are effectively confined in a smaller volume around the rods than in the perpendicular configuration, which causes an entropic penalty. This suggests that the entropy of the counterions has a crucial role in determining the equilibrium configuration of the system.

4 Stability of the raft-like structures

The formation of scaffold-like meta-stable structures during the aggregation of rod-like polyelectrolytes has similarities to the raft-like structures observed experimentally in solutions of F-actin rods with multivalent salt [15]. Since we observe that in an intermediate range of salt concentrations the system is likely to be trapped in meta-stable states on its way to equilibrium, the question naturally arises as to how this finding might have relevance to experiments on highly charged rod-like polyelectrolytes such as F-actin in the presence of multivalent salt. The formation of aggregates from single filaments distributed randomly in the solution as the initial configuration is controlled by a time scale that has two components, namely the time that takes the filaments to find each other through diffusion and the time that takes to overcome energetic barriers [23]. Since the diffusion component of the characteristic relaxation time could be substantial for dilute solutions, having long relaxation times does not necessarily mean that large energetic barriers impede the formation of equilibrium structures [23, 24]. To eliminate the diffusion component of the aggregation time and focus specifically on the energetic barriers in the dynamics of the system, we can study the evolution of already made complexes towards equilibrium. While strictly speaking this corresponds to a different kinetic pathway, one can imagine that a similar process of disentanglement of the interacting filaments will be followed in the aggregation kinetics, on the way to equilibrium. Therefore, measuring the relaxations times of already formed structures could provide a direct quantitative measure of the kinetics of the meta-stable state of the system. To this end, we study systematically the stability and time evolution of raft-like aggregates under various conditions.

We construct raft-like structures of stiff polyelectrolytes at different salt concentrations, and fix them at the beginning of the simulation (see Fig. 2 a) while the counterions and the salt ions are allowed to fluctuate. After the equilibration

of the free ions, we release the constraints on the polyelectrolyte rods and follow the evolution of the system. We find that in the low salt concentration regime thermal fluctuations destroy these structures in a short time. In fact, in this regime, there is not enough salt in the system for like-charge attraction between polyelectrolytes to appear and the electrostatic repulsion between the rods make such structures unstable. In the high salt concentration regime also the raft-like structures have a fast evolution and considerably short life time. In this regime mutually perpendicular rods slide against each other in a short time and the structure changes to bundles of parallel rods.

In the regime with intermediate salt concentration, however, the system has a different evolution. In this regime we find that the raft-like structures are considerably long-lived and it takes a long time for the fluctuations to destroy them. The system finally finds the lower free energy state in which bundles of parallel polyelectrolytes are formed. In this regime, the stability of raft-like structures increases with increasing salt concentration. A time lapse view of the system with $N_p = 9$ rods is shown in Fig. 2.

To help quantify the stability of the raft-like structures, we study the dependence of the evolution time of the structures towards bundles of parallel polyelectrolytes, as a function of the size of these structures while keeping the volume density of the filaments constant (by increasing the size of the simulation box with increasing number of filaments). The evolution time t_e is defined as the time it takes for a raft-like structure containing N_p polyelectrolytes to change to bundles of polyelectrolytes; for example the time interval between snapshots a and f of Fig. 2. The evolution time t_e as a function of the number of polyelectrolytes in the raft-like structure N_p is shown in Fig. 8a. The data points in this figure are obtained by averaging over five different runs of the system. In this figure, $N_p = 9$ corresponds to three mutually perpendicular layers and each layer contains three parallel rods (see Fig. 2). Similarly, $N_p = 15, 20, 25, 30, 40$ respectively correspond to 3, 4, 5, 6 and 8 layers and each layer contains

five parallel rods.

The characteristic evolution time t_e can be thought of as the time it takes for the raft-like structure to disentangle the filaments that strongly interact with each other via frustrated electrostatic interactions, and as can be seen in Fig. 8a it increases with increasing the size of the raft-like structure N_p . The increase is faster than linear, and can be approximated as a power law with an exponent of about 2.7 (see the inset of Fig. 8a for a log-log plot of t_e versus N_p), although the numerical data are not over a sufficiently large domain so that the power law nature can be verified. The characteristic relaxation time of the system as a function of the number of filaments (for a fixed volume density of single filaments) can be used to estimate the N_p dependence of the energy barrier (or activation energy) E_a for the transition between the raft-like structure and the equilibrium structure. Assuming a form of $t_e(N_p) = t_0 e^{E_a(N_p)/k_B T}$, where t_0 is a microscopic time scale that does not depend on the number of filaments, we can calculate relative changes in the activation energy as shown in Fig. 8b. While the plot in Fig. 8b clearly shows that the energy barrier increases with the number of filaments, more studies are necessary to determine whether this trend will continue or ultimately level off for systems with considerably larger number of filaments.

Using the estimate for the microscopic time scale $\tau_0 = 1.3$ ps, we find that for 9 rods the relaxation time is ~ 1 ns and for 40 rods it is ~ 0.1 μ s. To make a crude estimate for the typical relaxation times corresponding to realistic experimental cases [15], we can extrapolate the empirical scaling law to $N_p \sim 10^7$, which yields $t_e \sim 10^7$ s. This estimate suggests that the time the system could be trapped in a meta-stable state could be considerably long compared to typical observations times, for a system like F-actin. Further studies are necessary to determine whether the super-linear increase of the relaxation time as a function of the number of filaments persists for such large numbers present in the experiments on F-actin.

5 Concluding Remarks

We have studied the aggregation of stiff polyelectrolytes in bulk solution in the presence of multivalent salt, and have observed spontaneous formation of orientationally ordered aggregates. Our results show that in a range of salt concentrations, when two polyelectrolyte rods are at separations where their effective interaction is considerable, they could prefer to be perpendicular while their interaction is attractive. In this range of salt concentrations, we have observed the formation of relatively long-lived scaffold-like structures of the polyelectrolytes in the bulk solution, for which the mode of evolution through to the bundles of parallel polyelectrolytes is considerably slower than the typical kinetic modes of the system. We have also observed that in the above-mentioned range of the salt concentrations already formed raft-like structures similar to the ones observed in Ref. [15] have longer life time than those in the high and low salt concentration regimes.

Our findings suggest that when multivalent salt concentration is enough for like-charge attraction between polyelectrolytes but is not so high that they join up in parallel configuration directly, formation of raft-like structures could be possible as a meta-stable state. In our model system, which contains a small number of polyelectrolytes, the transition from the meta-stable state to the lower free energy state of bundles of parallel polyelectrolytes occur over a finite observable time. This evolution time, however, is observed to increase rapidly with the system size. This means that in a real experimental system with a large number polyelectrolytes involved in such a raft-like structure, it will be extremely difficult for the system to find the state with lower free energy in which the polyelectrolytes form dense bundles of parallel polyelectrolytes. In other words, our studies suggest that the experimentally observed raft-like structures might be meta-stable states with life times that are far larger than the experimentally available observation time. Further studies on larger systems and over longer simulation times are needed to fully verify this proposition, and characterize the nature of the intermediate

scaffold-like regime.

It is a great pleasure to acknowledge stimulating discussions with Gerard Wong.

References

- [1] C. Holm, P. Kekicheff, R. Podgornik, *Electrostatic Effects in Soft Matter and Biophysics*, (Kluwer, Dordrecht, 2001); Y. Levin, *Rep. Prog. Phys.*, 2002, **65**, 1577; H. Boroudjerdi, Y. -W. Kim, A. Naji, R. R. Netz, X. Schlagberger, A. Serr, *Phys. Rep.*, 2005, **416**, 129.
- [2] F. Oosawa, *Biopolymers*, 1968, **6**, 1633.
- [3] L. Guldbrand, L. G. Nilsson, L. Nordenskiöld, *J. Chem. Phys.*, 1986, **85**, 6686.
- [4] J. Israelachvili, *Intermolecular and Surface Forces*, (Academic, London, 1992) 2nd ed.
- [5] B.-Y. Ha, A. J. Liu, *Phys. Rev. Lett.*, 1997, **79**, 1289.
- [6] N. Gronbech-Jensen, R. J. Mashl, R. F. Bruinsma, W. M. Gelbart, *Phys. Rev. Lett.*, 1997, **78**, 2477.
- [7] M.J. Stevens, *Phys. Rev. Lett.*, 1999, **82**, 101.
- [8] R. Golestanian *et al.*, *Phys. Rev. Lett.*, 1999, **82**, 4456; R. Golestanian and T.B. Liverpool, *Phys. Rev. E*, 2002, **66**, 051802; O.V. Zribi *et al.*, *Europhys. Lett.*, 2005, **70**, 541; *Phys. Rev. E*, 2006, **73**, 031911; T.E. Angelini *et al.*, *Proc. Natl. Acad. Sci. U.S.A.*, 2006, **103**, 7962.
- [9] B. I. Shklovskii, *Phys. Rev. Lett.*, 1999, **82**, 3268.
- [10] V. A. Bloomfield, *Biopolymers*, 1991, **31**, 1471.
- [11] J. X. Tang and P. A. Janmey, *J. Biol. Chem.*, 1996, **271**, 8556.
- [12] R. Podgornik, D. Rau, V. A. Parsegian, *Biophys. J.*, 1994, **66**, 962.
- [13] A. Naji, A. Arnold, C. Holm, R.R. Netz, *Europhys. Lett.*, 2004, **67**, 130.
- [14] H. Lodish, A. Berk, S. L Zipursky, P. Matsudaria, D. Baltimore, J. Darnell, *Molecular Cell Biology*, (Freeman, New York, 2007), 6th Ed.
- [15] G.C.L. Wong, A. Lin, J. X. Tang, Y. Li, P. A. Janmey, C. R. Safinya, *Phys. Rev. Lett.*, 2003, **91**, 018103.
- [16] H. Fazli, R. Golestanian, and M.R. Kolehchi, *Phys. Rev. E*, 2005, **72**, 011805.
- [17] H. Fazli, R. Golestanian, P.L. Hansen, and M.R. Kolehchi, *Europhys. Lett.*, 2006, **73**, 429.
- [18] M. Konieczny and C.N. Likos, *Soft Matter*, 2007, **3**, 1130.
- [19] I. Borukhov, R. F. Bruinsma, *Phys. Rev. Lett.*, 2001, **87**, 158701.
- [20] K. Lee, I. Borukhov, W. M. Gelbart, A. J. Liu, M. J. Stevens, *Phys. Rev. Lett.*, 2004, **93**, 128101.
- [21] I. Borukhov, R. F. Bruinsma, W. M. Gelbart, A. J. Liu, *Proc. Natl. Acad. Sci. U.S.A.*, 2005, **102**, 3673.
- [22] M. Sayar, C. Holm, *Europhys. Lett.*, 2007, **77**, 16001.
- [23] H. Fazli, R. Golestanian, *Phys. Rev. E*, 2007, **76**, 041801.
- [24] G.H. Lai, O.V. Zribi, R. Coridan, R. Golestanian, and G.C.L. Wong, *Phys. Rev. Lett.*, 2007, **98**, 187802.
- [25] H. J. Limbach, A. Arnold, B. A. Mann, C. Holm, *Comp. Phys. Communications*, 2006, **174**, 704.
- [26] G. S. Grest, K. Kremer, *Phys. Rev. A*, 1986, **33**, 3628.
- [27] B. Dünweg and K. Kremer, *Phys. Rev. Lett* **66**, 2996 (1991).
- [28] H. M. Harreis, A. A. Kornyshev, C. N. Likos, H. Löwen, and G. Sutmann, *Phys. Rev. Lett.* **89**, 018303 (2002); H. M. Harreis, C. N. Likos, and H. Löwen, *Biophys. J.* **84**, 3607 (2003).

Fig. 1 Snapshots of the system containing $N_p = 9$ polyelectrolytes in solution with 3-valent salt concentration $c_{3:1} = 0.5$ as a function of time. +3 salt ions are shown by golden (light) spheres, +1 counterions by red (dark), and -1 salt ions by gray spheres. Corresponding times of snapshots in units of τ_0 : (a) 10, (b) 25, (c) 40, (d) 55, (e) 70, (f) 85. Aggregates of polyelectrolytes with scaffold-like structures can be seen in the snapshots e and f. Finally, all of the polyelectrolytes form a single bundle (last configuration is not shown here).

Fig. 2 Snapshots from evolution of a raft-like structure formed by $N_p = 9$ polyelectrolytes in the presence of 3-valent salt of concentration $c_{3:1} = 0.5$. The positive 3-valent salt ions are shown by golden (light) spheres and the negative salt ions and counterions are not shown for clarity. Corresponding times of snapshots in units of τ_0 : (a) initial configuration before equilibration of the ions, (b) 50, (c) 250, (d) 400, (e) 550, (f) 700.

Fig. 3 Potential of mean force between two rods as a function of θ at different values of R and salt concentration $c_{3:1}$ (see the schematic configuration of the rods in the inset of the middle plot). The legends of the other two plots are the same as that of the rightmost plot.

Fig. 4 Potential of mean force between two parallel rods (see the schematic configuration of the rods in the inset) as a function of center-to-center separation R for different concentrations of 3-valent salt. It can be seen that at salt concentrations $c_{3:1} \geq 0.2$ there is attraction between two parallel polyelectrolytes.

Fig. 5 Potential of mean force between two

perpendicular rods (schematic configuration of the rods is shown in the inset) as a function of R at different concentrations of 3-valent salt. The size of the circles on the $c_{3:1} = 0$ curve shows the size of error bars for all our data points. Note that the potential is not shown for $R < 1.6\sigma$ where the excluded volume interaction takes over and generates a strong repulsion.

Fig. 6 Preferred angle θ_p and interaction type between two charged rigid rods which are fixed on two parallel plates of separation R , in different regions of $c_{3:1} - R$ plane (see the schematic configuration of the rods in the middle plot of Fig. 3).

Fig. 7 Ensemble average of the interaction energy (Lennard-Jones + Coulomb) per particle between two rods with their separation fixed at $R = 2.5\sigma$ as a function of θ with no added salt. Inset: potential of mean force between the same two rods. The different trends of the two curves shows that the entropy of counterions has an important role in the orientation of the rods.

Fig. 8 (a) Evolution time of raft-like structures to bundles of parallel polyelectrolytes as a function of N_p , number of polyelectrolytes forming these structures. Error bars are obtained from averaging over five runs of the simulation with different random number sequences. Inset: Log-log plot of t_e versus N_p and a line with the slope of 2.7 (dashed line). (b) Activation energy extracted from (a) as a function of N_p .

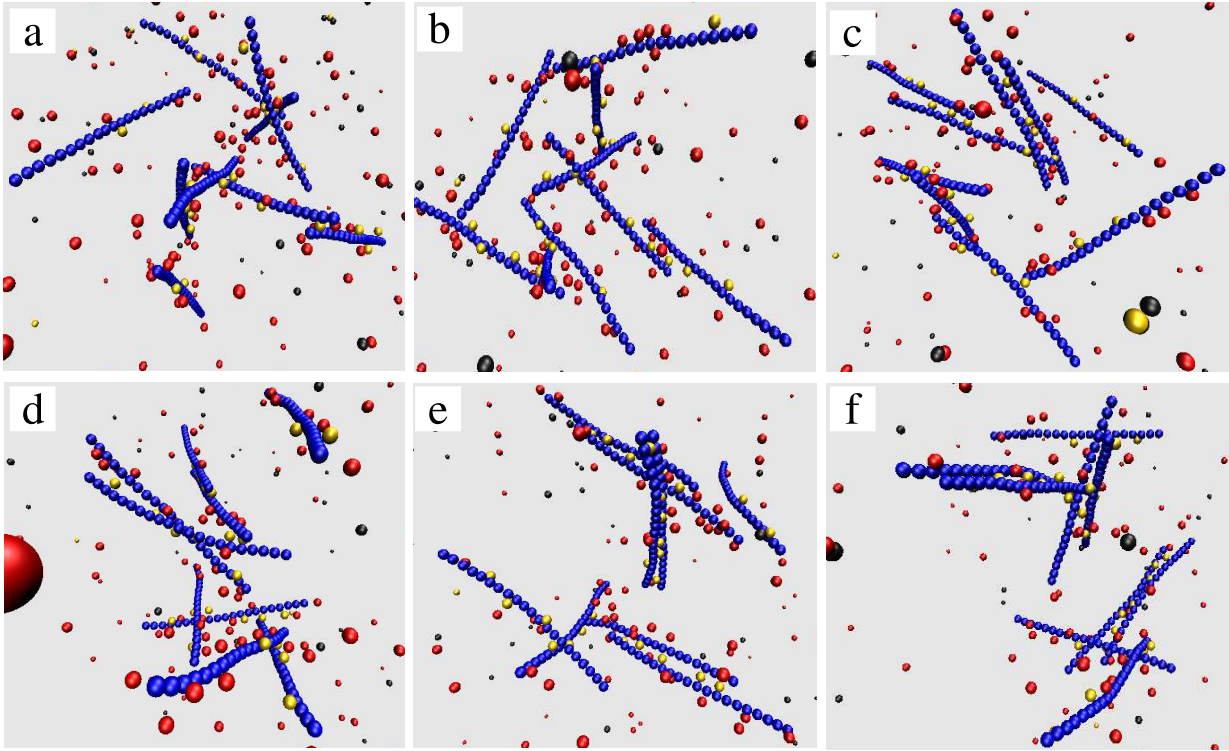


Figure 1: Snapshots of the system containing $N_p = 9$ polyelectrolytes in solution with 3-valent salt concentration $c_{3:1} = 0.5$ as a function of time. +3 salt ions are shown by golden (light) spheres, +1 counter-ions by red (dark), and -1 salt ions by gray spheres. Corresponding times of snapshots in units of τ_0 : (a) 10, (b) 25, (c) 40, (d) 55, (e) 70, (f) 85. Aggregates of polyelectrolytes with scaffold-like structures can be seen in the snapshots e and f. Finally, all of the polyelectrolytes form a single bundle (last configuration is not shown here).

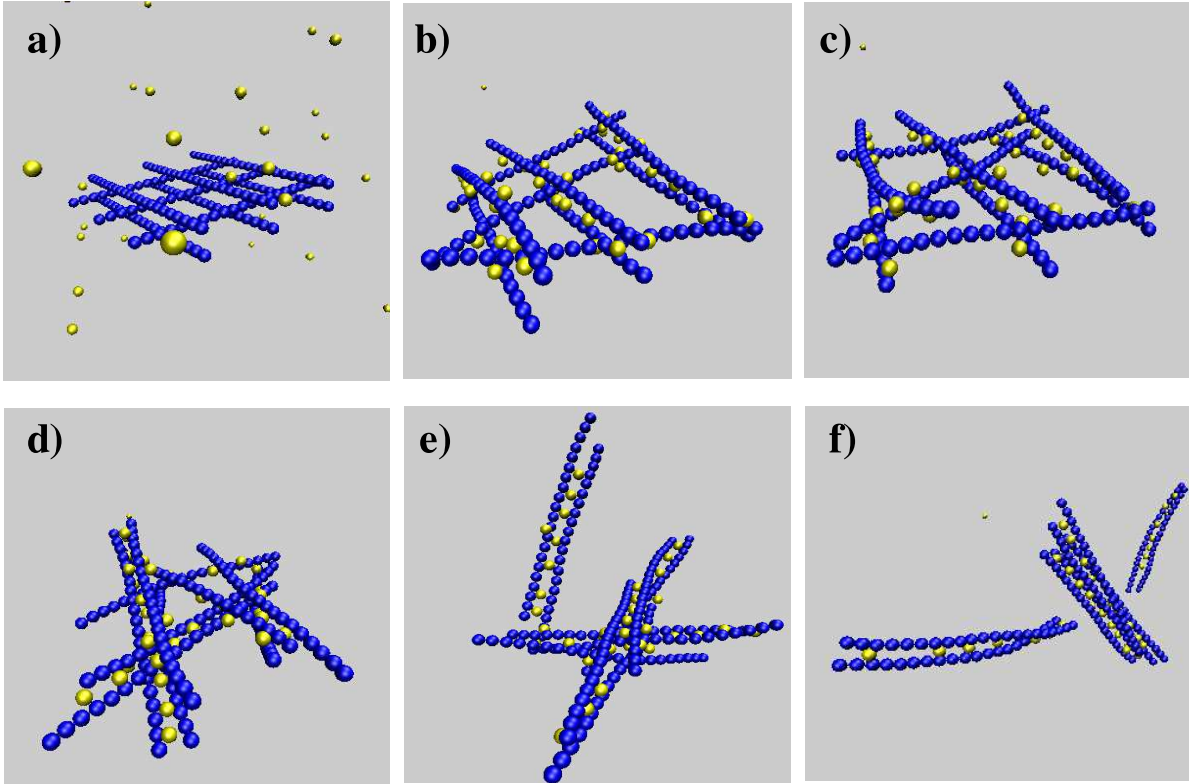


Figure 2: Snapshots from evolution of a raft-like structure formed by $N_p = 9$ polyelectrolytes in the presence of 3-valent salt of concentration $c_{3:1} = 0.5$. The positive 3-valent salt ions are shown by golden (light) spheres and the negative salt ions and counterions are not shown for clarity. Corresponding times of snapshots in units of τ_0 : (a) initial configuration before equilibration of the ions, (b) 50, (c) 250, (d) 400, (e) 550, (f) 700.

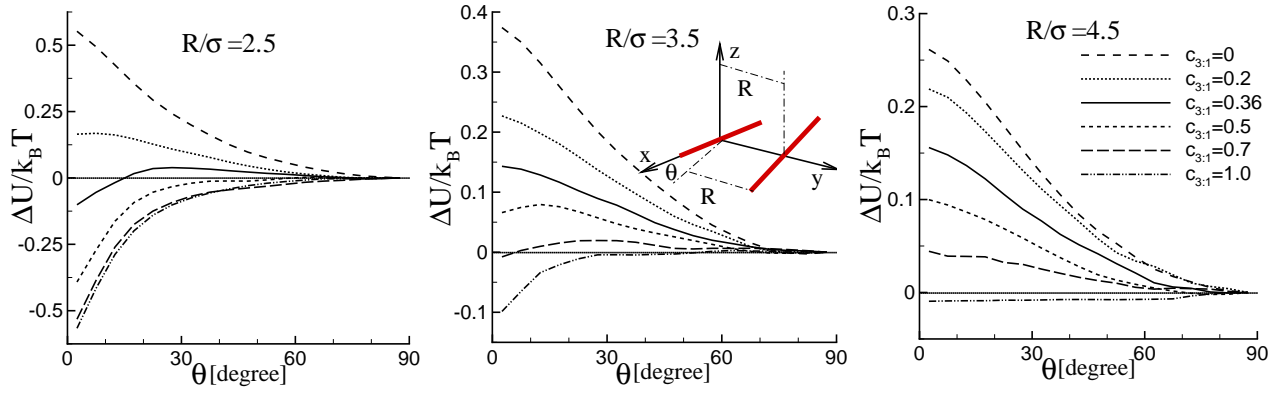


Figure 3: Potential of mean force between two rods as a function of θ at different values of R and salt concentration $c_{3:1}$ (see the schematic configuration of the rods in the inset of the middle plot). The legends of the other two plots are the same as that of the rightmost plot.

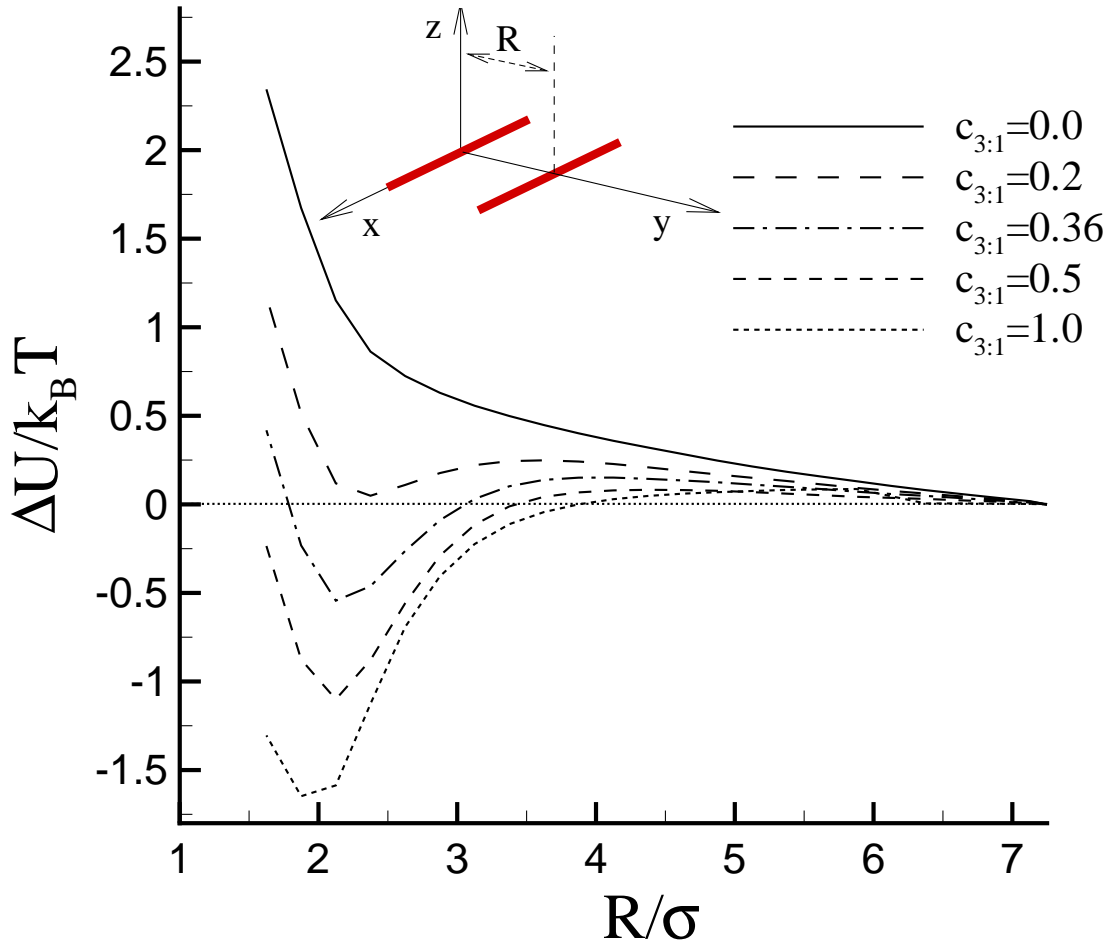


Figure 4: Potential of mean force between two parallel rods (see the schematic configuration of the rods in the inset) as a function of center-to-center separation R for different concentrations of 3-valent salt. It can be seen that at salt concentrations $c_{3:1} \geq 0.2$ there is attraction between two parallel polyelectrolytes.

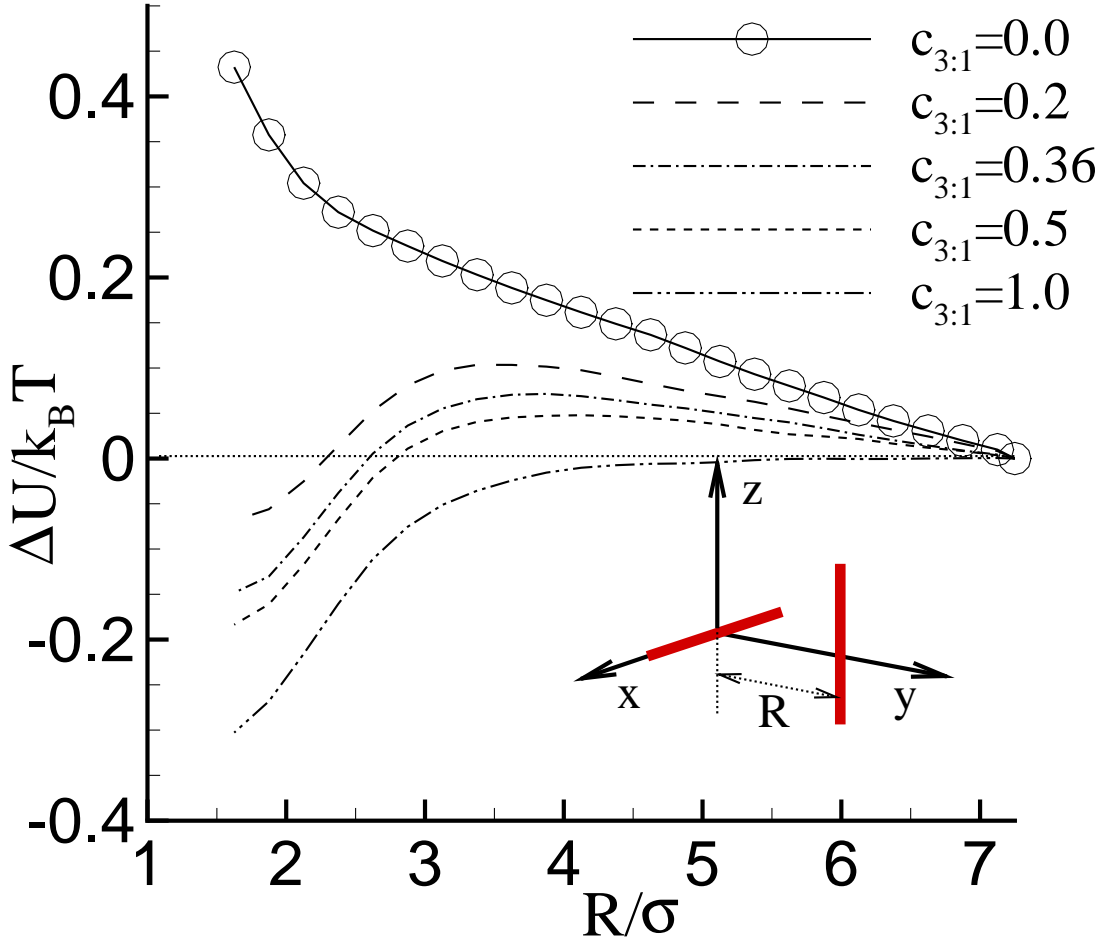


Figure 5: Potential of mean force between two perpendicular rods (schematic configuration of the rods is shown in the inset) as a function of R at different concentrations of 3-valent salt. The size of the circles on the $c_{3:1} = 0$ curve shows the size of error bars for all our data points. Note that the potential is not shown for $R < 1.6\sigma$ where the excluded volume interaction takes over and generates a strong repulsion.

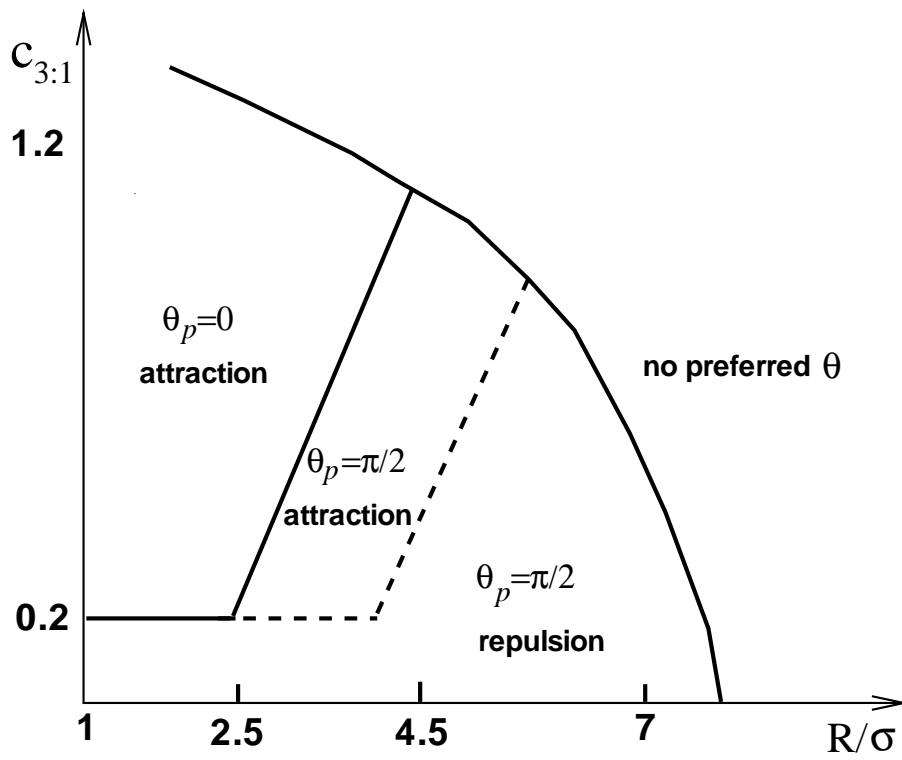


Figure 6: Preferred angle θ_p and interaction type between two charged rigid rods which are fixed on two parallel plates of separation R , in different regions of $c_{3:1} - R$ plane (see the schematic configuration of the rods in the middle plot of Fig. 3).

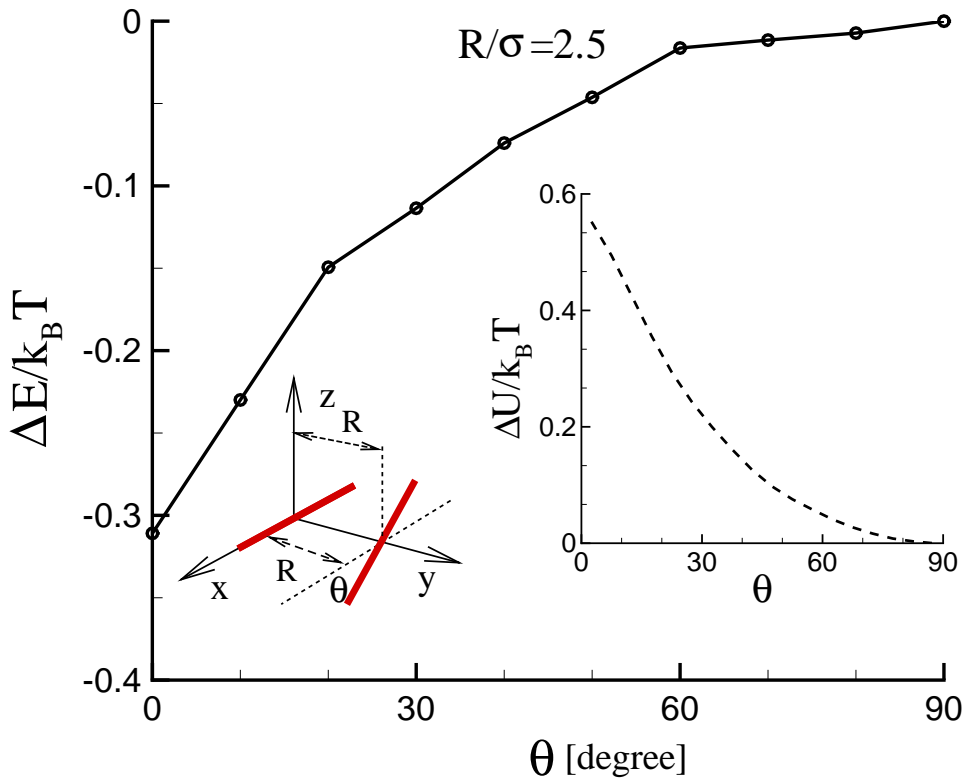


Figure 7: Ensemble average of the interaction energy (Lennard-Jones + Coulomb) per particle between two rods with their separation fixed at $R = 2.5\sigma$ as a function of θ with no added salt. Inset: potential of mean force between the same two rods. The different trends of the two curves shows that the entropy of counterions has an important role in the orientation of the rods.

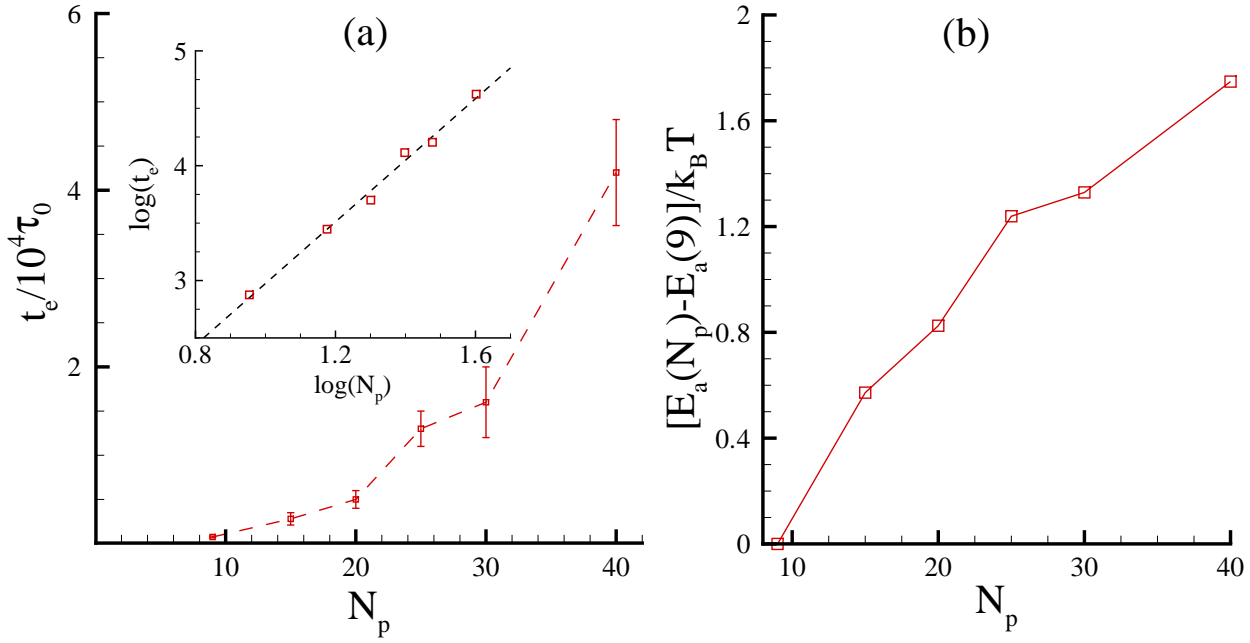


Figure 8: (a) Evolution time of raft-like structures to bundles of parallel polyelectrolytes as a function of N_p , number of polyelectrolytes forming these structures. Error bars are obtained from averaging over five runs of the simulation with different random number sequences. Inset: Log-log plot of t_e versus N_p and a line with the slope of 2.7 (dashed line). (b) Activation energy extracted from (a) as a function of N_p .